Three-Phase Unbalanced Load Flow Tool for Distribution Networks

Demirok, Erhan; Kjær, Søren Bækhøj; Sera, Dezso; Teodorescu, Remus

Published in:
Proceedings of the 2nd International Workshop on Integration of Solar Power Systems

Publication date:
2012

Document Version
Early version, also known as pre-print

Three-Phase Unbalanced Load Flow Tool for Distribution Networks

Erhan Demirok, Søren B. Kjær, Dezso Sera, and Remus Teodorescu

***Abstract*—This work develops a three-phase unbalanced load flow tool tailored for radial distribution networks based on Matlab®. The tool can be used to assess steady-state voltage variations, thermal limits of grid components and power losses in radial MV-LV networks with photovoltaic (PV) generators where most of the systems are single phase. New ancillary service such as static reactive power support by PV inverters can be also merged together with the load flow solution tool and thus, the impact of the various reactive power control strategies on the steady-state grid operation can be simply investigated. Performance of the load flow solution tool in the sense of resulting bus voltage magnitudes is compared and validated with IEEE 13-bus test feeder.**

***Index Terms*—Load flow, LV network, PV integration, voltage unbalance.**

I. Introduction

POWER balance between generation-consumption and power quality are two essential targets on the overall electrical power system to be continuously maintained within the most economical way of delivery. Assuming that power balance is guaranteed by the central power generators under varying power demand, network components will be exposed to certain amount of current and voltage stresses and will generate losses in the network. Load flow study here plays an important role as a tool to assess these stresses in the steady-state domain.

Minimum requirements of a load flow solution will vary depending on whether power system under study is transmission or distribution network. Exemplifying this, power flow in transmission networks is usually balanced and the network structures likely contain meshed or looped lines. Therefore, it is sufficient to represent transmission systems as single phase components. On the other hand, distribution networks typically accommodate single/two/three-phase loads and four-wire cables/lines so that load flow solutions shall handle unbalanced power flow with 3-phase modeling of network components. Since distribution networks mostly operate in radial structure, more straightforward and convergence guaranteed load flow solutions can be employed by taking advantage of this structure.

In general, this work was inspired by MatDyn tool [1]-[2] which focuses on dynamical analysis of power systems, MATPOWER [3] and PSAT [4] that were developed to run balanced load flow/optimal load flow on single-phase equivalent circuits especially for transmission networks. However, in reality, rooftop PV installations have usually widespread usage in residential areas through single-phase connections. Therefore, regarding of more realistic network analysis, a 3-phase load flow script can allow more precise estimation of PV hosting capacity in unbalanced cases.

Most of the load flow solution methods proposed so far in the literature can be generalized in three groups:

- Gauss-like methods [5]-[8],
- Newton-Raphson (NR) based methods [9]-[14], and
- Backward-forward sweep (BFS) based methods [15]-[17].

Concerning precise estimation of PV hosting capacity of distribution networks, primary requirements can be summarized as

1. All class of loads including 2-phase, single-phase and constant impedance, constant power, constant current types or their combination shall be represented in a load flow study for more realistic investigation,
2. Load flow solver shall take into account of asymmetric layouts and mutual coupling situation of lines, cables and transformers,
3. Time series simulation is necessary for daily, monthly and yearly assessments. Therefore, the solver shall be fast enough to run load flow for one year period with certain time steps, e.g. every 15 minutes,
4. Any user-defined functions and ancillary services of PV inverters should be integrated into the load flow solver without need of another program,
5. Load flow solver should be flexible to enable statistical study on the resulting data.

Although the first three requirements can be provided by some commercial power system simulation packages (PowerFactory, NetBas, CYMDIST, etc.), a MATLAB® based unbalanced load flow solver has been developed in this work based on the various state of the art publications from the literature and thus, it can be used for the assessment of maximum PV hosting capacity of distribution networks.

This work was financially supported by Aalborg University-Danfoss Solar Inverters A/S partnership. Any opinions, findings, and conclusions or recommendations expressed in this material are those of the authors and do not necessarily reflect those of Danfoss Solar Inverters A/S.

E. Demirok, D. Sera and R. Teodorescu are with Department of Energy Technology, Aalborg University, 9220 Denmark (e-mail: ede@et.aau.dk).

S. B. Kjaer is with Danfoss Solar Inverters A/S, Sønderborg 6400 Denmark.

A generalized functional block diagram is depicted in Fig. 1. In the following sections, the load flow solution concept is given firstly and a bus and branch numbering technique based on breadth-first search algorithm is described. Next, power systems modeling of some components (lines/cables, transformers, shunt capacitors, loads) are briefly provided as 3-phase representations. Load flow solver developed in Matlab® is validated on IEEE 13-bus test networks.

II. Load Flow Solution Concept

BFS method is selected here as the most suitable solver due to its simplicity and better convergence performance compared to Gauss-like and NR based methods under the assumption of radial network structures. The main advantage of BFS algorithm is the straightforward implementation of Kirchoff's current and voltage laws on the feeders. In this way, branch currents and bus voltages are updated by traversing between the root (source or slack) bus and end buses in iterative way (Fig. 2). Specifying initial bus voltages and nominal ratings of shunt components (loads, capacitor banks, and generators), backward sweep updates branch currents by summation of child branches and shunt currents from end nodes toward the root node. Similarly, starting from the specified root bus voltage and knowing the branch currents from the previous backward sweep, bus voltages are updated from the root node towards end nodes by means of voltage drops along the branches. Thus single iteration of backward-forward sweep is completed. If line charging capacitances are neglected, two general equations as referred to Fig. 2 for backward and forward sweep can be written as (1)-(2) respectively.

$$J_i^{tbus} = J_i^{fbus} = \underbrace{I_i}_{\substack{shunt \\ currents}} + \underbrace{\sum J_{subbranch}^{fbus}}_{\substack{sub-branch \\ currents}} \tag{1}$$

$$V_i = V_{i-1} - J_i^{fbus} \cdot Z_{branch} \tag{2}$$

Consecutive backward-forward sweep is terminated when the difference of resulting bus voltage magnitudes based on the previous iteration are less than predetermined tolerance value.

It should be noticed that BFS procedure must follow the branch current and bus voltage updates in a proper sequence. Therefore, bus and branch ordering will play important role to obtain a correct network solution.

III. Bus and Branch Numbering Technique

BFS concept as shown above briefly converges to a unique and accurate solution as long as bus-branch connection structure for the whole network is provided. Given *(m-1)* branches will form an *m*-bus network. Each branch located between two predefined buses ("*from bus*" and "*to bus*") is the only relevant input data to the load flow solver. The aim is to assign unique numbers to buses in such a way that backward and forward sweeps can follow the sequential branches systematically between the root bus and end buses. Breadth-first and depth-first search methods are the simplest graph algorithms to achieve this goal [19] and they are both classified as uninformed search methods. As distinct from depth-first method, breadth-first search method explores all the nodes reachable from the root node in a graph. Accordingly, it is applicable on mesh structured distribution networks because of producing inherently "breadth-first tree" form from the looped graphs.

Bus and branch numbering can be integrated into the breadth-first search algorithm. As proposed in [18], a three-index scheme that assigns branch level (*l*), branch index (*m*) and bus index (*n*) to each bus is systematically introduced in (*l,m,n*) order. The main idea behind the bus numbering technique is that buses located on the same feeder will be identified with the same branch level *l*, and the buses on the other child sub-branches will have level of *l+1*. If multiple sub-branches within the same level exist in the network, then buses on the same level of sub-branches can be uniquely identified by lateral index *m*. Lastly, the third index of *n* refers to the nth bus on the branch (*l,m*). An example of bus numbering is illustrated in Fig. 3.

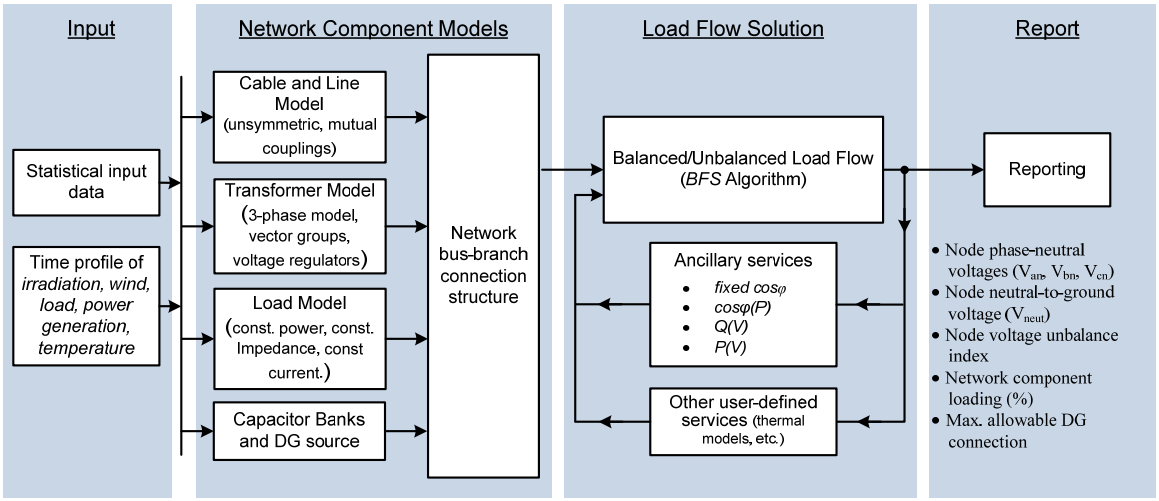

Fig. 1. Generalized functional block diagram of the load flow method developed in Matlab®

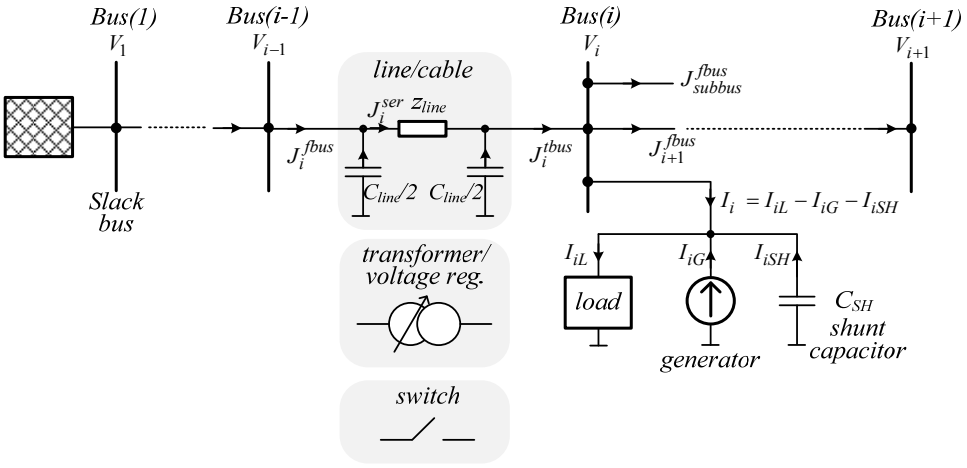

Fig. 2. Two-bus and single-line representation of distribution networks for the solution of *BFS* algorithm

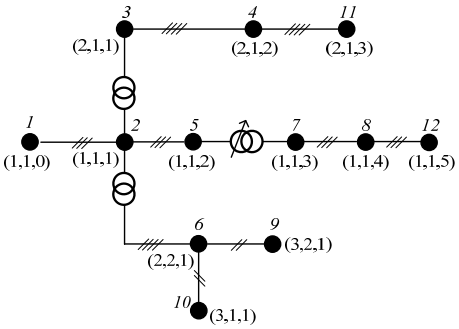

Fig. 3. An example of bus numbering for a radial structure

IV. Component Modeling

A. 3-Phase Distribution Line/Cable Model

Unsymmetrical spacing between phase conductors without transposition is the most common property of distribution lines. It is likely to see unequal voltage drops among the phases, even though power flow is balanced along a distribution line. For this reason, unbalanced three-phase load flow solution will require accurate modeling of distribution lines for the steady-state voltage analysis. Additionally, in reality, loads and distributed generators are usually connected between line and neutral terminals for 3-phase 4-wire systems. However, most of the distribution network analysis disregards the phase to neutral voltages so that voltage unbalance is miscalculated. Therefore, neutral-to-earth voltage (NEV) at each node can be estimated here for multi-grounded neutral system. In case of unbalanced load flow condition, the return current will be divided into neutral and earth circuit. Share amount of return currents among neutral and earth circuit mainly depends on the neutral conductor and grounding electrode impedances. On account of this, unlike Kersting's phase impedance matrix [20], neutral conductors can be explicitly represented here in the series impedance of lines/cables. Since the equivalent shunt impedance of lines/cables (e.g. line charging capacitor) has negligible impact on voltage drop in distribution networks, only series impedances will be considered here.

Carson's line equations have been used to generate a series impedance matrix for the given line/cable configuration in this work (Appendix). Fig. 4 depicts typical 3-phase 4-wire overhead line and its equivalent circuit. Voltage drop along a line based on the primitive impedance matrix (A.7) as provided in Appendix can be calculated as:

$$\begin{bmatrix} V_a(i) \\ V_b(i) \\ V_c(i) \\ V_n(i) \end{bmatrix} = \begin{bmatrix} V_a(i-1) \\ V_b(i-1) \\ V_c(i-1) \\ V_n(i-1) \end{bmatrix} - \underbrace{\begin{bmatrix} z_{aa} & z_{ab} & z_{ac} & z_{an} \\ z_{ba} & z_{bb} & z_{bc} & z_{bn} \\ z_{ca} & z_{cb} & z_{cc} & z_{cn} \\ z_{na} & z_{nb} & z_{nc} & z_{nn} \end{bmatrix}}_{Z_{line}} \cdot \begin{bmatrix} J_a(i) \\ J_b(i) \\ J_c(i) \\ -J_n(i) \end{bmatrix} \quad (3)$$

where

$V_{a,b,c,n}(i)$ are the phase and neutral voltages of the i^{th} node as referenced to their own local earth,

$J_{a,b,c,n}(i)$ are the incoming branch phase and neutral currents of the i^{th} node.

In order to solve voltage drop in (3), phase and neutral

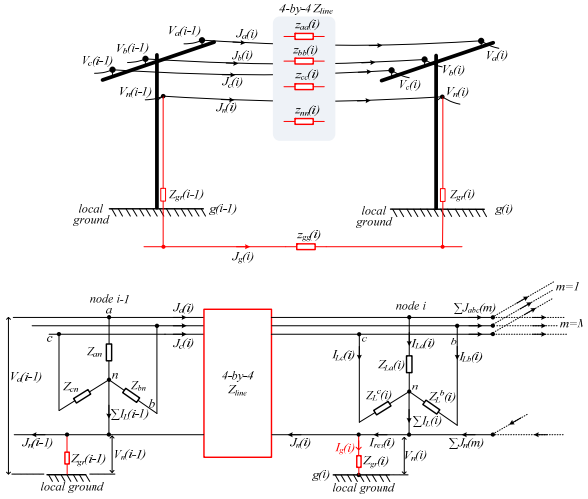

Fig. 4. Typical 3-phase 4-wire overhead line segment (upper); and its generalized circuit representation (bottom)

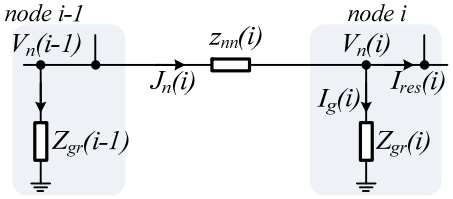

Fig. 5. Closer look on the neutral and grounding circuit. Current directions are matched with Carson's circuit

branch currents have to be determined accurately during backward sweep. For the computation of neutral branch current J_n, three constraints are introduced as in (4)-(6) and as referred to Fig. 5 [22].

$$I_g(i) = V_n(i) / Z_{gr}(i) \tag{4}$$

$$J_n(i) = I_g(i) + I_{res}(i) \tag{5}$$

and the last constraint is defined by the last row of (3):

$$V_n(i-1) - V_n(i) = \begin{bmatrix} z_{an} & z_{bn} & z_{cn} \end{bmatrix} \cdot \begin{bmatrix} J_a \\ J_b \\ J_c \end{bmatrix} + z_{nn} \cdot J_n = \begin{bmatrix} z_{in} \end{bmatrix} \begin{bmatrix} J_{abc} \end{bmatrix} + z_{nn} \cdot J_n \tag{6}$$

By combining (4)-(6), the branch neutral current is provided in terms of neutral voltage of parent node, grounding impedance of local node, incoming branch phase currents, and residual current that is calculated by summation of all sub-branches:

$$J_n(i) = \frac{V_n(i-1) - \left[z_{in}(i)\right] \cdot \left[J_{abc}(i)\right] + I_{res}(i) \cdot Z_{gr}(i)}{Z_{gr}(i) + z_{nn}(i)} \tag{7}$$

where I_{res} is the residual current and computed as:

$$I_{res}(i) = \sum_{k=\{a,b,c\}} I_{L,k}(i) + \sum_{k=\{a,b,c\}} I_{sh,k}(i) + \sum_{m \in M} J_n(m) \tag{8}$$

M is the set of sub-branches that branch off the i^{th} node, $I_L(i)$ and $I_{sh}(i)$ denote load and shunt capacitor currents in respectively; absorbed by the i^{th} node.

Phase currents along the branch are determined as given in (9) during backward sweep and finally, the required branch currents will be completed to compute voltage drops in (3).

$$\begin{bmatrix} J_a(i) \\ J_b(i) \\ J_c(i) \end{bmatrix} = \begin{bmatrix} I_{L,a}(i) + I_{sh,a}(i) \\ I_{L,b}(i) + I_{sh,b}(i) \\ I_{L,c}(i) + I_{sh,c}(i) \end{bmatrix} - \begin{bmatrix} \left(\frac{S_{gen,a}}{V_a(i) - V_n(i)} \right)^* \\ \left(\frac{S_{gen,b}}{V_b(i) - V_n(i)} \right)^* \\ \left(\frac{S_{gen,c}}{V_c(i) - V_n(i)} \right)^* \end{bmatrix} + \begin{bmatrix} \sum_{m \in M} J_a(m) \\ \sum_{m \in M} J_b(m) \\ \sum_{m \in M} J_c(m) \end{bmatrix} \tag{9}$$

$S_{gen}(i)$ is the apparent power of constant PQ generator connected at i^{th} node.

B. Load Model

Compared to transmission networks, various balanced and unbalanced load types exist in distribution networks according to number of phases (1- or 3-phase) and connection types (delta or star). Moreover, in the sense of electricity consumption characteristics, constant power, constant current, constant admittance or any combination must be performed for the realistic load models. If a measured load profile is available with certain time intervals, then the class of constant power may be preferred selection among the other load characteristics. For some cases, only load density along a line is specified in terms of kVA/km and usually assumed to be uniformly distributed for the simplicity. In accordance with this, loads can be further classified as spot and uniformly distributed loads. Fig. 6 shows wye- and delta-connected spot loads while Table I summarizes model equations where I^k, V^k represent load phase currents and voltages at k^{th} iteration, respectively. From the specified rated power (S_L) and rated voltage levels (V_{rated}) of loads, the nominal current (I_{nom}) and nominal admittance (y^{nom}) values per phase are determined to be used in Table I:

$$I_{L,a}^{nom} = \left(\frac{S_{L,a}}{V_a^{rated}} \right)^*, \quad y_{L,a}^{nom} = \frac{\left(S_{L,a}\right)^*}{\left|V_a^{rated}\right|^2} \rightarrow \text{for } Y_g$$

$$I_{L,ab}^{nom} = \left(\frac{S_{L,ab}}{V_a^{rated} - V_b^{rated}} \right)^*, \quad y_{L,ab}^{nom} = \frac{\left(S_{L,ab}\right)^*}{\left|V_a^{rated} - V_b^{rated}\right|^2} \rightarrow \text{for } \Delta \tag{10}$$

Matrix T used in Table I provides transformation of the phase currents into the line currents which are eventually necessary to compute branch currents.

$$T = \begin{bmatrix} 1 & 0 & -1 \\ -1 & 1 & 0 \\ 0 & -1 & 1 \end{bmatrix}$$

Without loss of generality, generator models considered in this work will be equivalent to negative constant power loads. Since most of the generators connected to MV and LV distribution networks operate in constant power mode.

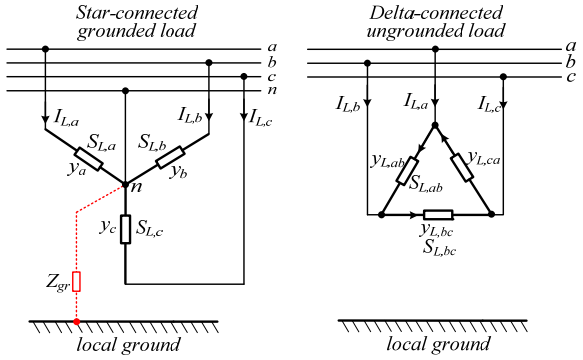

Fig. 6. Wye (left) and delta-connected (right) spot loads

C. Shunt Capacitor Model

Shunt capacitors are located on the distribution networks in order to help regulating voltage levels and compensate reactive power demand. From the modeling point of view, their implementation in load flow simulation is similar to the constant admittance load model.

D. 3-Phase Two-Winding Transformer Model

Regarding of European distribution networks, 20-kV or 10-kV MV distribution networks are commonly engaged to 60-kV or 110-kV sub-transmission networks through the substations that usually contain delta-delta (*D-D*) connection type of transformers with on-load tap changers.

TABLE I
SPOT LOAD MODEL EQUATIONS

	Constant Complex Power	Constant Current	Constant Admittance (impedance)
Grounded wye-connected load	$\begin{bmatrix} I^k_{L,a} \\ I^k_{L,b} \\ I^k_{L,c} \end{bmatrix} = \begin{bmatrix} \left(\frac{S_{L,a}}{V^{k-1}_a - V^{k-1}_n}\right)^* \\ \left(\frac{S_{L,b}}{V^{k-1}_b - V^{k-1}_n}\right)^* \\ \left(\frac{S_{L,c}}{V^{k-1}_c - V^{k-1}_n}\right)^* \end{bmatrix}$	$\begin{bmatrix} I^k_{L,a} \\ I^k_{L,b} \\ I^k_{L,c} \end{bmatrix} = \begin{bmatrix} I^{nom}_{L,a} \\ I^{nom}_{L,b} \\ I^{nom}_{L,c} \end{bmatrix}$	$\begin{bmatrix} I^k_{L,a} \\ I^k_{L,b} \\ I^k_{L,c} \end{bmatrix} = \begin{bmatrix} y^{nom}_{L,a} \cdot V^{k-1}_a \\ y^{nom}_{L,b} \cdot V^{k-1}_b \\ y^{nom}_{L,c} \cdot V^{k-1}_c \end{bmatrix}$
Delta-connected load	$\begin{bmatrix} I^k_{L,a} \\ I^k_{L,b} \\ I^k_{L,c} \end{bmatrix} = T \cdot \begin{bmatrix} \left(\frac{S_{L,ab}}{V^{k-1}_a - V^{k-1}_b}\right)^* \\ \left(\frac{S_{L,bc}}{V^{k-1}_b - V^{k-1}_c}\right)^* \\ \left(\frac{S_{L,ca}}{V^{k-1}_c - V^{k-1}_a}\right)^* \end{bmatrix}$	$\begin{bmatrix} I^k_{L,a} \\ I^k_{L,b} \\ I^k_{L,c} \end{bmatrix} = T \cdot \begin{bmatrix} I^{nom}_{L,ab} \\ I^{nom}_{L,bc} \\ I^{nom}_{L,ca} \end{bmatrix}$	$\begin{bmatrix} I^k_{L,a} \\ I^k_{L,b} \\ I^k_{L,c} \end{bmatrix} = T \cdot \begin{bmatrix} y^{nom}_{L,ab} \cdot \left(V^{k-1}_a - V^{k-1}_b\right) \\ y^{nom}_{L,bc} \cdot \left(V^{k-1}_b - V^{k-1}_c\right) \\ y^{nom}_{L,ca} \cdot \left(V^{k-1}_c - V^{k-1}_a\right) \end{bmatrix}$

On the other hand, 400-V 3-phase 4-wire secondary distribution feeders branch off MV feeders along delta - grounded wye (*D-Yg*) transformers with off-load tap changers.

Modeling of 3-phase distribution transformers in phase coordinates requires more attention due to the possibility of having ill-conditioned matrices for certain type of transformers. Basically, two modeling approaches exist in the literature. Direct approach is based on application of Kirchoff's voltage and current loops for both primary and secondary circuit of the transformer [23]. This transformer modeling approach is developed only for *BFS* load flow algorithm. The other method generates nodal admittance matrices that represent 3-phase transformer configurations [24]-[27]. The operability of nodal admittance matrix-based modeling approach is more extensive and it is able to support any load flow algorithm. However, matrix singularity problem of some transformer configurations leads to limited implementation of nodal admittance matrix approach.

In this work, nodal admittance matrix-based transformer modeling tailored for *BFS* load flow algorithm has been developed. Matrix singularity problem is stressed and then fixed by means of introducing additional constraints on the node admittance matrix of transformer. Although modeling of *D-Yg* type step-down transformer will be presented here, the same modeling methodology can be further applied to the other connection types of two-winding transformers.

It will be assumed that the secondary side line-to-line voltages are lagging the primary side line-to-line voltages by 30º which represents the prevalent class of transformers (*D-Yg1*) in Europe (Fig. 7). In this respect, secondary side terminal currents will be also lagging the primary side terminal currents by 30º. As another assumption, magnetizing impedance of the transformer is sufficiently high to be neglected as compared to leakage impedance. Furthermore, each primary-secondary phase windings are assumed to be formed by separate and identical single-phase transformers (this is why it is also called as 3-phase transformer bank). This makes cross couplings between the primary and secondary windings zero and simplifies mathematical modeling of the transformers with tolerable errors. Additionally, mutual admittance (*m*) between each phase will be assumed to equal to winding leakage admittances (*y*=*m*).

As a first step to computation of node admittance matrix, primitive admittance matrix (Y_{prim}) that represents relationship between phase voltages and currents at primary and secondary circuits is formed. Then, connection matrices (*C* and *D*) transforms the phase quantities into the node quantities, thus, the resulted node voltages and currents can be directly used in load flow solution.

$$\underbrace{C^T \cdot I_{ph}}_{I_{node}} = \underbrace{D \cdot Y_{prim} \cdot C}_{Y_{node}} \cdot V_{node} \tag{11}$$

Each transformer configuration will have its own primitive admittance and connection matrices. For this reason, it will be necessary to store the resulting node admittance matrices for various transformer configurations

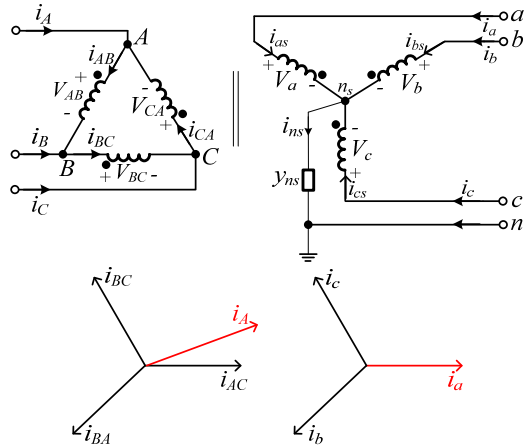

Fig. 7. D-Yg1 transformer bank connection and its positive-sequence current phasor diagram based on [23]

in load flow solution tool. The primitive impedance matrix Y_{prim}, the connection matrices (C, D) and the node admittance matrix Y_{node} are given in Appendix based on Fig. 7.

Concerning the *BFS* load flow algorithm, phase currents at primary side are computed in terms of secondary side currents and voltages during backward step. Similarly, secondary side terminal voltages are expressed in terms of the primary side voltages and currents during forward step. This is summarized in Table II based on (A.14).

However, it can be investigated from (A.14) that sub-matrices of $\overline{Y}_{pp}$ and $\overline{Y}_{ps}$ are not invertible and only two of the three equations in these sub-matrices are linearly independent. For this reason, additional constraints must be introduced in such a way that singularities of $\overline{Y}_{pp}^{-1}$ and $\overline{Y}_{ps}^{-1}$ are avoided.

The first constraint is introduced by non-existence of zero sequence voltage at delta side of the transformer so that the sum of primary side line-to-line voltages will be zero. The other constraint comes with a relationship between the currents and voltages at grounded-wye side of the transformer using (A.14). Thus, as referred to (A.14), if secondary currents are sum up,

$$\sum I_s = i_a + i_b + i_c = -y\cancel{\left(V_{AB} + V_{BC} + V_{CA}\right)} - y\left(V_{ag} + V_{bg} + V_{cg}\right) \tag{12}$$

then the forward sweep equation in Table II is updated by imposing (12) into the its third row as:

$$\underbrace{\begin{bmatrix} - & - & - \\ y & y & y \end{bmatrix}}_{\overline{Y}_{ps}} \underbrace{\begin{bmatrix} V_{ag} \\ V_{bg} \\ V_{cg} \end{bmatrix}}_{V_s} = \underbrace{\begin{bmatrix} - \\ -\sum i_s \end{bmatrix}}_{I_p} - \underbrace{\begin{bmatrix} - & - & - \\ 0 & 0 & 0 \end{bmatrix}}_{\overline{Y}_{pp}} \cdot V_p \tag{13}$$

and new updated $\overline{Y}_{ps}$ becomes invertible matrix at all. On the other hand, regarding of the backward step; $\overline{Y}_{sp}$ was already invertible so there is no need of introducing constraints for the backward sweep.

TABLE II
TRANSFORMER MODEL VALID FOR ALL CONFIGURATIONS: CURRENT AND VOLTAGE COMPUTATION FOR *BFS* STEPS

Backward step	Forward step
Step 1. $V_p = \left(\overline{Y}_{sp}\right)^{-1} \cdot \left(I_s - \overline{Y}_{ss} V_s\right)$	Step 1. $V_s = \left(\overline{Y}_{ps}\right)^{-1} \cdot \left(I_p - \overline{Y}_{pp} V_p\right)$
Step 2. $I_p = \overline{Y}_{pp}\overline{V}_p + \overline{Y}_{ps}\overline{V}_s$	

E. Computation of Network Active Power Losses

Regardless of what computation method is used, total branch losses of distribution networks can be calculated once bus voltages and branch currents all over the network are obtained accurately after running a load flow simulation. Although branch impedance can be used to estimate active power losses by means of I^2R, this method gives rise to inaccurate solution due to phase mutual couplings in 3-phase systems. In general, loss dissipated along a branch is equivalent to the difference between branch entering and branch outgoing power.

$$\begin{aligned} S_{loss,k} &= S_{fbus,k} - S_{tbus,k} \\ &= \begin{bmatrix} V^a_{fbus,k} \cdot \left(I^a_{fbus,k}\right)^* \\ V^b_{fbus,k} \cdot \left(I^b_{fbus,k}\right)^* \\ V^c_{fbus,k} \cdot \left(I^c_{fbus,k}\right)^* \end{bmatrix} - \begin{bmatrix} V^a_{tbus,k} \cdot \left(I^a_{tbus,k}\right)^* \\ V^b_{tbus,k} \cdot \left(I^b_{tbus,k}\right)^* \\ V^c_{tbus,k} \cdot \left(I^c_{tbus,k}\right)^* \end{bmatrix} \end{aligned} \tag{14}$$

where $S_{fbus,k}$ denotes apparent power entering into the k^{th} branch and $S_{tbus,k}$ refers to the apparent power leaving the k^{th} branch.

V. VALIDATION OF THE DEVELOPED LOAD FLOW TOOL

IEEE 13-bus test network is used to examine modeling performance of various components such as cables and lines with diverse configurations, all kind of loads, shunt capacitors, voltage regulator and transformers. Fig 8 illustrates the 13-bus test network. Minor modification has been applied on the original test network as following:

1) Delta-connected, constant power (Y-PQ) uniformly distributed load situated between nodes 2 and 3 has been removed from the original network. Since most of the distributed load had been connected to *phase c*, new result will overestimate the *phase c* voltage.
2) In the original test network, a switch and an additional node exist between node 3 and 11. Since load flow results published by IEEE consider only "on" state of the switch, it doesn't make sense to include it in this work.

Modeling data can be found in [28]. The on load tap changer (OLTC) is positioned at [10 8 11] for phase *a*, *b*, *c* respectively in such a way that minimum voltage level in the network becomes higher than 0.95 p.u. Fig. 9 shows the 3-phase line-to-ground voltage profile of the network provided by the developed load flow tool. However, in this case, the nearest nodes to OLTC will experience severe voltage boosting. Therefore, increasing tap positions further levels cannot be accepted although maximum tap position of the OLTC is 16 per phase. Therefore, connecting shunt capacitors at far end nodes can help mitigating this problem for long distribution feeders. The results obtained by the developed load flow simulation have been compared with the results from Radial Distribution Analysis Package (RDAP) [29] as shown in Fig. 9. Phase *c* voltages from both results are overestimated due to removal of the uniformly distributed load in the modified network. Overall voltage mismatches take place in the acceptable level of 0.1-2 % as referenced to IEEE and RDAP simulation results.

Fig. 10 illustrates comparison of resulting node voltages as line-to-ground and line-to-neutral together. Considering line-to-neutral voltages, lightly loaded phase *b* moves to emergency condition and relevant tap setting of OLTC or the rating of shunt capacitors connected to phase *b* must be re-adjusted to prevent this overvoltage situation. Another point is the effect of grounding impedance on the neutral voltage. As depicted in Fig. 11, neutral voltages do not vary

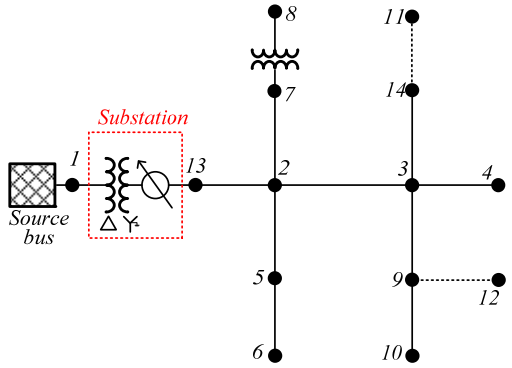

Fig. 8. IEEE 13-bus network [28]. Solid lines represent overhead lines; dashed lines refer to underground cables

substantially as grounding impedance is increased to 100 ohms. It is obvious that slightly shifting up of neutral voltages is observed due to the fact that higher grounding impedance forces more return currents to flow through the neutral conductor.

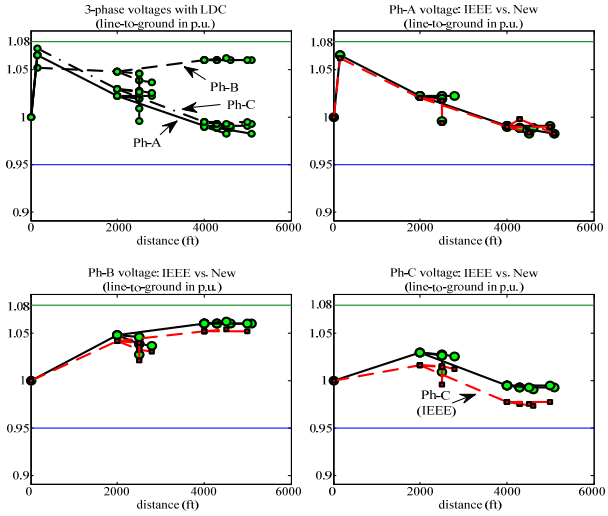

Fig. 9. Line-to-ground voltage profile of IEEE 13-bus network with OLTC

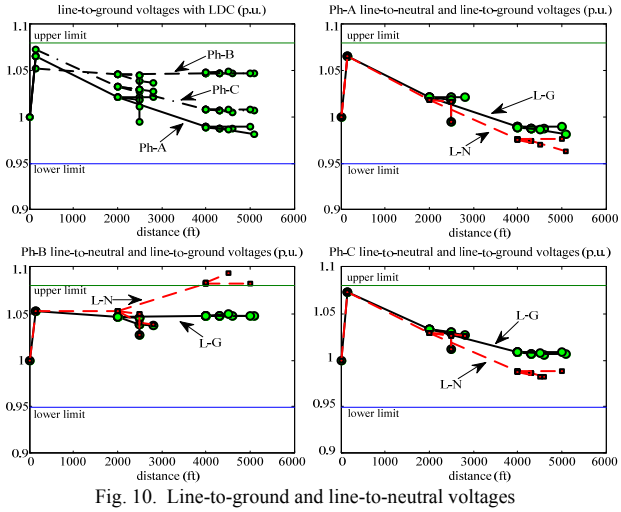

Fig. 10. Line-to-ground and line-to-neutral voltages

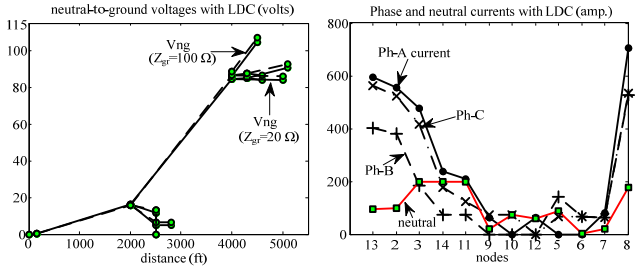

Fig. 11. Neutral-to-ground voltages and branch currents

VI. Conclusion

Since the load flow solution methods are well documented in the literature, one of the attentions here is to investigate and establish appropriate technics special for the distribution networks. Owing to Matlab®'s powerful computational performance and ready-to-use functions, the tool becomes flexible by allowing users to develop their own special model functions (thermal model of components, ancillary services, detailed generator models, etc.) and any special network analysis (statistical load flow solution, yearly energy and loss analysis, etc.). The tool will be practiced on a realistic LV network in order to estimate its maximum PV hosting capacity with different unbalanced scenarios.

New load flow tool has been successfully implemented on 3-phase 4-wire circuits. Thus, besides on phase voltage unbalance, neutral-to-ground voltages and neutral currents can also be assessed for multi-grounded neutral systems.

VII. Appendix

A. Carson's Equations for Line Modeling

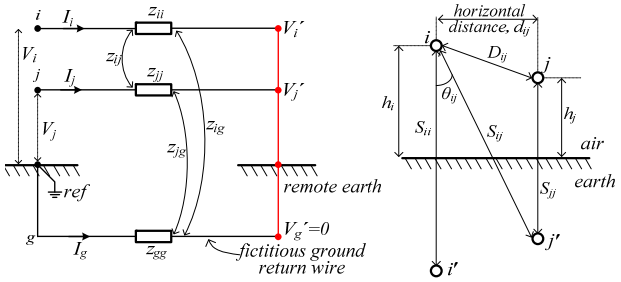

Fig. A. Carson's two-conductor circuit with ground return (left); physical layout of two conductors with ground return (right)

Fig. A illustrates Carson's line circuit and two-conductor line spacing layout with their image conductors. For unbalanced power flow situation, it is obvious that current injections will return to the source through the earth (fictitious ground wire). When receiving end nodes are shorted at the remote earth together, self- and mutual-impedances of conductors can be determined by knowing sending node voltages (V_i,V_j) and currents flowing along the conductors (I_i, I_j).

$$\begin{bmatrix}\Delta V_i\\ \Delta V_j\\ \Delta V_g\end{bmatrix}=\begin{bmatrix}V_i-V_i'\\ V_j-V_j'\\ V_g-V_g'\end{bmatrix}=\begin{bmatrix}z_{ii} & z_{ij} & z_{ig}\\ z_{ij} & z_{jj} & z_{jg}\\ z_{ig} & z_{jg} & z_{gg}\end{bmatrix}\cdot\begin{bmatrix}I_i\\ I_j\\ I_g\end{bmatrix} \quad (A.1)$$

where $V_i' = V_j' = V_g'$, $V_g = 0$ and $I_i + I_j + I_g = 0$. Thus reduced voltage equation for the i^{th} conductor becomes:

$$V_i = \left(z_{ii} - 2\cdot z_{ig} + z_{gg}\right)\cdot I_i + \left(z_{ij} - z_{ig} + z_{gg} - z_{gj}\right)\cdot I_j = \overline{z}_{ii}\cdot I_i + \overline{z}_{ij}\cdot I_j \quad \text{(A.2)}$$

If simplified Carson's equations are used based on [20]-[21], then self- and mutual impedance of conductor including ground effects thus becomes:

$$\overline{z}_{ii} = r_i + \pi^2 fG + j4\pi fG\cdot\left(\ln\left(S_{ii}/GMR_i\right) + 5.7974 + \ln\sqrt{\rho/f}\,/h_i\right) \quad \text{(A.3)}$$

$$\overline{z}_{ij} = \pi^2 fG + j4\pi f\cdot G\cdot\left(\ln\left(S_{ij}/D_{ij}\right) + 6.4906 + \ln\sqrt{\rho/f}\,/S_{ij}\right) \quad \text{(A.4)}$$

where

$\overline{z}_{ii}$ is the self-impedance of i^{th} conductor in Ω/km or Ω/mile,

$\overline{z}_{ij}$ is the mutual-impedance between i^{th} and j^{th} conductor in Ω/km or Ω/mile,

r_i is the resistance of i^{th} conductor in Ω/km or Ω/mile,

f is the system frequency in Hz,

h_i is the height of i^{th} conductor in meter ($S_{ii}=2h_i$),

GMR_i is the geometric mean radius of i^{th} conductor in meter,

ρ is the resistivity of earth in Ω-meters,

S_{ij} is the distance between conductor i and conductor j' (image of conductor j) in meter,

D_{ij} is the distance between conductor i and conductor j in meter

$G=10^{-4}$ in Ω/km or $0.1609347\cdot10^{-3}$ in Ω/mile

and

$$P_{ij} \cong \pi/8$$

$$Q_{ij} \cong -0.0386 + \frac{1}{2}\left(\ln\left[2/2\cdot\left(2.8099\cdot10^{-3}\right)\right] + \ln\sqrt{\rho/f}\,/h_i\right) \quad \text{(A.5)}$$

$$r_{ij} = 2.8099\cdot10^{-3}\cdot S_{ij}\cdot\sqrt{f/\rho} \quad \text{(A.6)}$$

After this point, the primitive series impedance matrix can be formed. It should be noticed that ground-related terms are already merged into the self- and mutual-impedances of phase and neutral conductors if Carson's equations are directly implemented [20]. Accordingly, the primitive series impedance matrix is given as:

$$z_{prim} = \begin{bmatrix} \overline{z}_{aa} & \overline{z}_{ab} & \overline{z}_{ac} & \overline{z}_{an} \\ \overline{z}_{ba} & \overline{z}_{bb} & \overline{z}_{bc} & \overline{z}_{bn} \\ \overline{z}_{ca} & \overline{z}_{cb} & \overline{z}_{cc} & \overline{z}_{cn} \\ \overline{z}_{na} & \overline{z}_{nb} & \overline{z}_{nc} & \overline{z}_{nn} \end{bmatrix} \quad \text{(A.7)}$$

B. Admittance Matrices for D-Yg1 Transformer

Based on Fig. 7, the primitive admittance matrix is written as following:

$$\begin{bmatrix} i_{CA} \\ i_{AB} \\ i_{BC} \\ i_{as} \\ i_{bs} \\ i_{cs} \\ i_{ns} \end{bmatrix} = \underbrace{\left[\begin{array}{ccc|ccc|c} y & & & -m & & & 0 \\ & y & & & -m & & 0 \\ & & y & & & -m & 0 \\ \hline -m & & & y & & & 0 \\ & -m & & & y & & 0 \\ & & -m & & & y & 0 \\ \hline 0 & 0 & 0 & 0 & 0 & 0 & y_{ns} \end{array}\right]}_{Y_{prim}} \begin{bmatrix} V_{CA} \\ V_{AB} \\ V_{BC} \\ V_{an} \\ V_{bn} \\ V_{cn} \\ V_{ns} \end{bmatrix} \quad \text{(A.8)}$$

where subscripts in big letters denote the primary side phase quantities and subscripts in small letters represent the quantities in secondary circuit. v_{ns} refers neutral grounding admittance. It should be noticed that ungrounded side terminal voltages are represented in line-to-line whereas grounded side terminal voltages are given in terms of line-to-ground voltages. The connection matrices C and D are:

$$\begin{bmatrix} V_{CA} \\ V_{AB} \\ V_{BC} \\ V_{an} \\ V_{bn} \\ V_{cn} \\ V_{ng} \end{bmatrix} = \underbrace{\left[\begin{array}{ccc|ccc|c} 0 & 0 & 1 & & & & 0 \\ 1 & 0 & 0 & & 0 & & 0 \\ 0 & 1 & 0 & & & & 0 \\ \hline & & & -1 & & & 1 \\ & 0 & & & -1 & & 1 \\ & & & & & -1 & 1 \\ \hline 0 & 0 & 0 & 0 & 0 & 0 & 1 \end{array}\right]}_{C} \begin{bmatrix} V_{AB} \\ V_{BC} \\ V_{CA} \\ V_{ag} \\ V_{bg} \\ V_{cg} \\ V_{ng} \end{bmatrix} \quad \text{(A.9)}$$

$$\begin{bmatrix} i_A \\ i_B \\ i_C \\ i_a \\ i_b \\ i_c \\ i_n \end{bmatrix} = \underbrace{\left[\begin{array}{ccc|ccc|c} -1 & 1 & 0 & & & & 0 \\ 0 & -1 & 1 & & 0 & & 0 \\ 1 & 0 & -1 & & & & 0 \\ \hline & & & 1 & & & 0 \\ & 0 & & & 1 & & 0 \\ & & & & & 1 & 0 \\ \hline & 0 & & -1 & -1 & -1 & 1 \end{array}\right]}_{D} \begin{bmatrix} i_{CA} \\ i_{AB} \\ i_{BC} \\ i_{as} \\ i_{bs} \\ i_{cs} \\ i_{ns} \end{bmatrix} \quad \text{(A.10)}$$

and, 7-by-7 node admittance matrix becomes:

$$Y_{node} = \left[\begin{array}{ccc|ccc|c} y & 0 & -y & -y & y & 0 & 0 \\ -y & y & 0 & 0 & -y & y & 0 \\ 0 & -y & y & y & 0 & -y & 0 \\ \hline 0 & 0 & -y & -y & & & y \\ -y & 0 & 0 & & -y & & y \\ 0 & -y & 0 & & & -y & y \\ \hline y & y & y & y & y & y & y_{ns} - 3y \end{array}\right] = \left[\begin{array}{c|c|c} Y_{pp} & Y_{ps} & Y_{pn} \\ \hline Y_{sp} & Y_{ss} & Y_{sn} \\ \hline Y_{np} & Y_{ns} & Y_{nn} \end{array}\right] \quad \text{(A.11)}$$

Further reduction can be applied on (A.11) since current entering into the internal neutral node (ns) is only supplied by the internal sum of phase currents and there is no external current injection to the internal neutral node. Therefore, the last row of Y_{node} can be rewritten as:

$$\left[\begin{array}{c} \\ \hline i_n = 0 \end{array}\right] = \left[\begin{array}{c|c|c} & & \\ \hline Y_{np} & Y_{ns} & Y_{nn} \end{array}\right] \begin{bmatrix} V_p \\ V_s \\ V_n \end{bmatrix}, V_n = -Y_{nn}^{-1}\left(Y_{np}V_p - Y_{ns}V_s\right) \quad \text{(A.12)}$$

V_p denotes $\begin{bmatrix} V_{AB} & V_{BC} & V_{CA} \end{bmatrix}^T$ and V_s is $\begin{bmatrix} V_{ag} & V_{bg} & V_{cg} \end{bmatrix}^T$. For example, when (A.12) is applied to the primary side current (top row of Y_{node}):

$$I_p = Y_{pp}V_p + Y_{ps}V_s + Y_{pn}V_n = \underbrace{\left(Y_{pp} - Y_{pn}Y_{nn}^{-1}Y_{np}\right)}_{Y11} \cdot V_p + \underbrace{\left(Y_{ps} - Y_{pn}Y_{nn}^{-1}Y_{ns}\right)}_{Y12} \cdot V_s \quad \text{(A.13)}$$

And if the same is repeated for the secondary currents, then generalized 6-by-6 reduced node admittance matrix can be obtained as

$$Y_{node} = \left[\begin{array}{c|c} Y11 & Y12 \\ \hline Y21 & Y22 \end{array}\right] = \left[\begin{array}{c|c} Y_{pp} - Y_{pn}Y_{nn}^{-1}Y_{np} & Y_{ps} - Y_{pn}Y_{nn}^{-1}Y_{ns} \\ \hline Y_{sp} - Y_{sn}Y_{nn}^{-1}Y_{np} & Y_{ss} - Y_{sn}Y_{nn}^{-1}Y_{ns} \end{array}\right]$$

$$= \left[\begin{array}{ccc|ccc} y & 0 & -y & -y & y & 0 \\ -y & y & 0 & 0 & -y & y \\ 0 & -y & y & y & 0 & -y \\ \hline m & m & n & n & m & m \\ n & m & m & m & n & m \\ m & n & m & m & m & n \end{array}\right]$$

where $m=y^2/(3y-y_{ns})$ and $n=y^2/(3y-y_{ns})-y$. For solidly grounded D-Yg1 transformer ($y_{ns} \to \infty$), the node admittance matrix becomes:

$$\lim_{y_{ns}\to\infty} Y_{node} = \left[\begin{array}{ccc|ccc} y & 0 & -y & -y & y & 0 \\ -y & y & 0 & 0 & -y & y \\ 0 & -y & y & y & 0 & -y \\ \hline 0 & 0 & -y & -y & & \\ -y & 0 & 0 & & -y & \\ 0 & -y & 0 & & & -y \end{array}\right] = \left[\begin{array}{c|c} \bar{Y}_{pp} & \bar{Y}_{ps} \\ \hline \bar{Y}_{sp} & \bar{Y}_{ss} \end{array}\right] \quad \text{(A.14)}$$

VIII. References

[1] MatDyn webpage [Online]. Available: http://www.esat.kuleuven.be/electa/teaching/matdyn/

[2] S. Cole and R. Belmans, "MatDyn, a new Matlab-based toolbox for power system dynamic simulation," *IEEE Trans. on Power Systems*, vol. 26, no. 3, pp. 1129-1136, August 2011.

[3] R.D. Zimmerman, C.E. Murillo-Sanchez, and D.D. Gan, "MATPOWER-A Matlab power system simulation package,". [Online]. Available: http://www.pserc.cornell.edu/matpower/

[4] L. Vanfretti and F. Milano, "The experience of PSAT as a free and open source software for power system education and research," *International Journal of Electrical Engineering Education*, vol. 47, no. 1, pp. 47-62, January 2010.

[5] H.E. Brown, G.K. Carter, H.H. Happ, and C.E. Person, "Power flow solution by impedance matrix iterative method," *IEEE Trans. On Power Apparatus and Systems*, vol. PAS-82, no. 65, pp. 1-10, April 1963.

[6] T.H. Chen, M.S. Chen, K.J. Hwang, P. Kotas, and E.A. Chebli, "Distribution system power flow analysis-A rigid approach," *IEEE Trans. On Power Delivery*, vol. 6, no. 3, pp. 1146-1152, July 1991.

[7] J.C.M. Vieira, W. Freitas, and A. Morelato, "Phase decoupled method for three phase power flow analysis of unbalanced distribution system," *IEE Proceedings of Generation, Transmission and Distribution*, vol. 151, no. 5, pp. 568-574, September 2004.

[8] K.P. Schneider, D. Chassin, Y. Chen, and J.C. Fuller, "Distribution power flow for smart grid technologies," *IEEE Power Systems Conference and Exposition*, pp. 1-7, Seattle, March 2009.

[9] J.E. Van Ness, "Iteration methods for digital load flow studies," *IEEE Trans. On Power Apparatus and Systems*, vol. 78, pp. 583-588, August 1959.

[10] W.F. Tinney and C.E. Hart, "Power flow solution by Newton's method," *IEEE Trans. on Power Apparatus and Systems*, vol. 78, pp. 583-588, August 1959.

[11] B. Stott and O. Alsac, "Fast decoupled load flow," *IEEE Trans. on Power Apparatus and Systems*, vol. Pas-93, no. 3, pp. 859-869, May 1974.

[12] R.D. Zimmerman and H.D. Chiang, "Fast decoupled power flow for unbalanced radial distribution systems," *IEEE Trans. on Power Systems*, vol. 10, no. 4, pp. 2045-2052, November 1995.

[13] P.A.N. Garcia, J.L.R. Pereira, S. Camerio, V.M. da Costa, and N. Martins, "Three-phase power calculations using the current injection method," *IEEE Trans. on Power Systems*, vol. 15, no. 2, pp. 508-514, May 2000.

[14] A. Abur, H. Singh, H. Liu, and W.N. Klingensmith, "Three phase power flow for distribution systems with dispersed generation," *14th Power Systems Computation Conference (PSCC)*, Sevilla, June 2002.

[15] W.H. Kersting and D.L. Mendive, "An application of ladder network theory to the solution of three-phase radial load flow problems," *IEEE PES General Winter Meeting*, January 1976.

[16] D. Shirmohammadi, H.W. Hong, A. Semlyen, and G.X. Luo, "A compensation based power flow method for weakly meshed distribution networks," *IEEE Trans. on Power Systems*, vol. 3, no. 2, pp. 753-762, May 1988.

[17] M.F. AlHajri and M.E. El-Hawary, "Exploiting the radial distribution structure in developing a fast and flexible radial power flow for unbalanced three-phase networks," *IEEE Trans. on Power Delivery*, vol. 25, no. 1, pp. 378-389, January 2010.

[18] R.D. Zimmerman, "Comprehensive distribution power flow: Modeling, formulation, solution algorithms and analysis," Ph.D. dissertation, Cornell University, January 1995.

[19] T.H. Cormen, *Introduction to Algorithms*, MIT Press, 2001.

[20] W.H. Kersting and R.K. Green, "The application of Carson's equation to the steady-state analysis of distribution feeders," *IEEE Power Systems Conference and Exposition (PSCE)*, Phoenix, March 2011.

[21] J.R. Carson, "Wave propagation in overhead wires with ground return," *Bell System Technical Journal*, pp. 539-554, 1926.

[22] E.R. Collins, J. Jiang, "Analysis of elevated neutral-to-earth voltage in distribution systems with harmonic distortion," *IEEE Trans. on Power Delivery*, vol. 24, no. 3, pp. 1696-1702, July 2009.

[23] W.H. Kersting, *Distribution System Modeling and Analysis*, CRC Press, 2007.

[24] T.H. Chen, M.S. Chen, T. Inouse, P. Kotas, E.A. Chebli, "Three-phase cogenerator and transformer models for distribution system analysis," *IEEE Trans. on Power Delivery*, vol. 6, no. 4, pp. 1671-1681, October 1991.

[25] S.S. Moorthy, D. Hoadley, "A new phase-coordinate transformer model for Ybus analysis," *IEEE Trans. on Power Systems*, vol. 17, no. 4, pp. 951-956, November 2002.

[26] P. Xiao, D.C. Yu, W. Yan, "A unified three-phase transformer model for distribution load flow calculations," *IEEE Trans. on Power Systems*, vol. 21, no. 1, pp. 153-159, February 2006.

[27] M.R. Irving, A.K. Al-Othman, "Admittance matrix models of three-phase transformer with various neutral grounding configurations," *IEEE Trans. on Power Systems*, vol. 18, no. 3, pp. 1210-1212, August 2003.

[28] [Online]. Available: http://ewh.ieee.org/soc/pes/dsacom/testfeeders/index.html

[29] RDAP User Manual, WH Power Consultants, Las Cruces, NM. Available: http://www.zianet.com/whpower